

## *Research prospects of satellite to satellite electron content*

R. LEITINGER and G. HOCHEGGER  
Institut für Geophysik, Astrophysik und Meteorologie,  
Universität Graz, A-8010 Graz, Austria

### ABSTRACT

The experimental set-up we deal with is reception onboard satellites in Low Earth Orbits (LEOs) of radio signals transmitted from satellites. Plasma propagation effects allow to derive the satellite to satellite electron content. The research prospects of this quantity can be divided into two branches: investigation of the ionosphere by making use of the occultation situation and investigation of the plasmasphere. We concentrate on the occultation branch and discuss evaluation possibilities and their prospects for the future. Classical inversion of the satellite to satellite electron content which is observed when the perigee of the radio link (ray) sinks from the orbital height of the receiver satellite to the ground or when it rises from ground occultation gives horizontally averaged height profiles of electron density. Assessment studies have been carried out to demonstrate the usefulness and the shortcomings of inversion results. Additional data or information about horizontal gradients of the electron density in the ionosphere offers several possibilities to improve the results. We discuss «Model Assisted Inversion» and «Tomographic Reconstruction».

**Key words:** LEO, Electron content, Occultation, Model Assisted Inversion, Tomographic Reconstruction.

### 1. INTRODUCTION

The electron content is the line integral of electron density between two points in a plasma. Various radio wave propagation effects give good (first order) approximations to electron content for a straight line drawn between a transmitter and a receiver (see, e.g., Leitinger (1998c) for a more recent historical overview). Of relevance for present time terrestrial applications in the ionosphere and the plasmasphere is the plasma influence on signal phase and pulse travel time. Both rely on the strong dispersion of a plasma which can be expressed through the frequency dependence of the refractive index,  $n$ . If

everywhere  $f \gg f_p$ , then the approximation  $n \doteq 1 - (1/2) (f / f_p)^2 = 1 - (1/2) A N_e / f^2$  is sufficiently accurate for assessment of both effects.  $N_e$  is the electron (number) density; the constant  $A = 80.6 \text{ m}^3 \text{ s}^{-2}$  if  $N_e$  is given in  $\text{m}^{-3}$ ,  $f$  in Hz. We use the plasma effects on the signals of Global Navigation Satellite Systems (GNSS – presently the US system GPS and the Russian system GLO-NASS) for examples.

If two carrier signals with different frequencies  $f_1$  and  $f_2$  are transmitted phase coherently (or can be reconstructed from spread spectrum transmissions) they can be derived from a common reference frequency,  $f_r$ , as  $f_1 = p f_r$ ,  $f_2 = q f_r$ ,  $p$  and  $q$  being integer numbers. The plasma influence on signal phase is proportional to the phase difference  $\psi = \varphi_1/p - \varphi_2/q$  if we use the designations  $\varphi_1$  and  $\varphi_2$  for the received signal phases. In a sloppy terminology  $\psi$  is often called «differential Doppler» (it is the «time integrated difference in Doppler shifts»). Since it is not possible to measure absolute phases and absolute phase differences it is necessary to add an «initial phase value»  $\Phi_0$  to gain  $\Phi = \psi + \Phi_0$ , the quantity which is proportional to electron content («calibration» or «phase ambiguity» problem, Leitinger et al., (1975)).

A coherent pulse modulation on two carrier signals enables to measure the plasma influence on pulse travel time (often called «pulse delay» or «group delay»). In principle, this effect is directly observable on GPS and GLONASS signals if the relative pulse delays of transmitter and receiver are known. There remains an uncertainty in equipment delays and since the effects are very small actual measurements can be strongly influenced by antenna effects, like reception of disturbing signals which have travelled over (slightly) different propagation paths («multipath problem»).

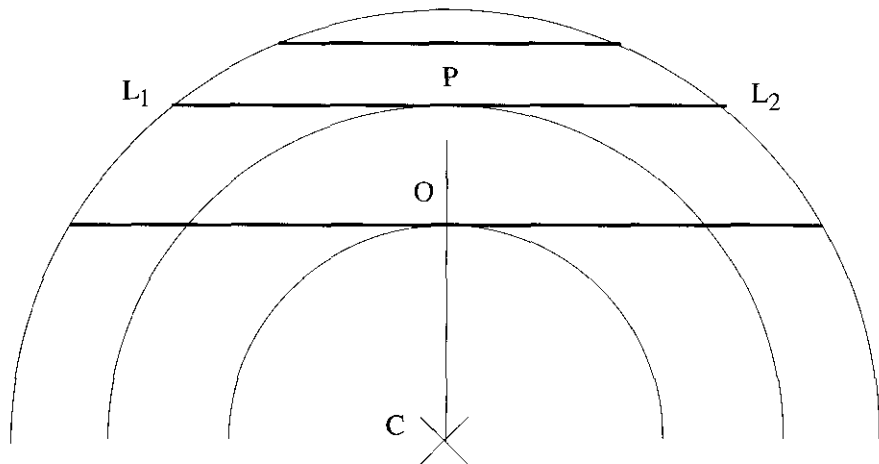


Figure 1. Occultation Configuration 1. C: center of Earth, O: ground occultation point (perigee of the ray which touches the ground), P: ray perigee,  $L_1$ : position of Leo 1,  $L_2$ : position of LEO 2.

There exist long and extensive experiences with satellite to ground electron content in general and most of the problems initially encountered when switching from other sources to GNSS have now been solved (see, e.g., Leitinger (1997, 1998c)).

With both radio beacon (transmitter) and receiver onboard satellites we have the possibility to derive satellite to satellite electron content. There are several different geometrical configurations. Excluding satellites with highly eccentric orbits it makes sense to distinguish satellites by their orbital heights. For sake of simplicity let us distinguish only between satellites in Low Earth Orbits (LEOs), satellites of the Global Navigation System type (GNSS) and geostationary satellites (GEOs) and let us assume that the LEO heights are below about 2000 km.

We discuss briefly the following configurations which have already found applications or application plans.

- C(1): Transmitters and receivers are onboard LEOs (Fig. 1),
- C(2): transmitters onboard GNSS satellites, receivers onboard LEOs (Fig. 2),
- C(3): transmitters onboard GEOs, receivers onboard LEOs.

With configuration C(1) we can distinguish two very useful cases.

C(1a): Transmitter satellite and receiver satellite follow each other and their distance remains comparatively small,

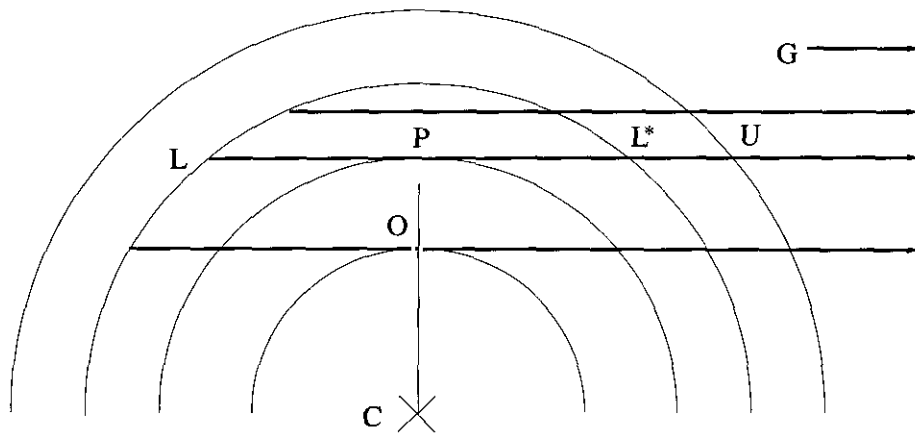


Figure 2. Occultation Configuration 2. C: center of Earth, O: ground occultation point (perigee of the ray which touches the ground), P: ray perigee, L: position of LEO, L\*: point on ray in the LEO height, U: point on ray in plasmasphere foot height.

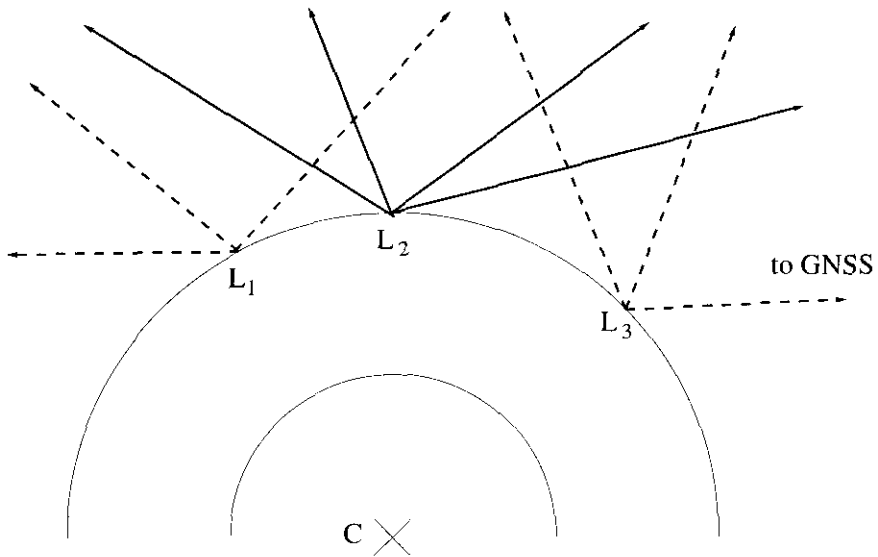


Figure 3. «Plasmasphere» Configuration. C: center of Earth,  $L_1$ ,  $L_2$ ,  $L_3$ : LEO positions.

**C(1b):** the two satellites are in the same orbital plane but orbit in opposite directions which leads to two close encounters of the satellites per period.

With configurations **C(2)** and **C(3)** we can distinguish between occultation scenarios (Fig. 3) and «plasmaspheric electron content» scenarios (Fig. 2). In the one case the satellite to satellite rays have perigees (points closest to the center of the Earth) with heights between the LEO orbit and the surface of the Earth and cross the ionosphere below the LEO orbit, in the latter case the rays cross the uppermost ionosphere (the ionosphere above the LEO orbit) and the plasmasphere.

## 2. OCCULTATION SCENARIOS

The ideal occultation scenario would be provided by configuration **C(1)** with nearly identical orbital heights of transmitter and receiver LEO. In this case the rays from the transmitter to the receiver cross only the ionosphere below the LEO height and «calibration» would be easy to gain because an occultation would start with satellite encounter and negligibly small satellite to satellite electron content if encounter is close enough or if the orbits are well above 1000 km. There is only faint hope that the LEO - LEO encounter configuration will find an application in the future. Its realization could be

used to gain simultaneously in-situ data from magnetically conjugate regions.

The occultation of GNSS signals received onboard LEO satellites leads to contamination of the observed electron contents with contributions from the regions between the LEO height and the GNSS height (uppermost ionosphere and plasmasphere).  $I_s = I_i + I_u + I_p$  ( $I_i$ : Ionospheric contribution from below the LEO height [ $L - L^*$  in Fig. 2],  $I_u$ : contribution from the uppermost ionosphere [Leo height to 2000 km],  $I_p$ : plasmaspheric contribution [2000 to 20000 km, the height of GNSS]) (see also Fig. 4).

With the LEO heights in consideration (around 800 km) the uppermost ionosphere poses more severe interpretation problems than the plasmaspheric contamination.

A GNSS receiver onboard a LEO satellite with an orbit inclination between about  $50^\circ$  and  $140^\circ$  provides around 1100 useful occultations per day based on an operational system of 48 GNSS satellites (24 GPS plus 24 GLONASS). Restriction to setting occultations and to GPS still leaves near 300 events per day. Of course, not all are suitable for ionospheric inversion. A good criterion can be derived from the ground projection of the ray perigees or from the duration of the (ionospheric) occultation event. We define the latter to be the transit time from the highest possible perigee (equal to the height of the LEO satellite) to the ground-grazing occultation (setting occultation) or from ground-grazing occultation to the highest possible perigee (rising occultation). Typical «good» occultation event durations range from about 5 to 9 minutes for a LEO height of 800 km.

The length of the ground projection of the ray perigee trajectory during an occultation event (termed «smearing length») can vary from a few kilometers to thousands of kilometers. (Theoretically, the lower limit is 0, but in practice this case is not realistic.) For inversion purposes a maximum smearing length of 550 km (or  $5^\circ$ ) is certainly acceptable. With LEO inclinations between  $50^\circ$  and  $140^\circ$ , about a quarter of the GNSS occultations have smearing lengths  $\leq 5^\circ$  (Leitinger, (1997), Høeg et al., (1995)).

## 2.1. Direct inversion

Direct inversion of occultation data gives horizontally averaged height profiles of electron density (Hajj et al., (1994), Hajj and Romans, (1998), Jakowski, (1999), Kursinski et al., (1996), Leitinger et al., (1997b), Leitinger and Kirchengast, (1997b), Rius et al., (1998), and others).

From a mathematical/numerical point of view with a straight line ray geometry the inversion of occultation data is a straightforward and numerically stable process. One gains a triangular design matrix and the equation system is solved by successive elimination starting with the electron density for the highest pixel (spherical shell). Well below the F2 region peak error accumulation can lead to meaningless results. Under nighttime conditions we should not

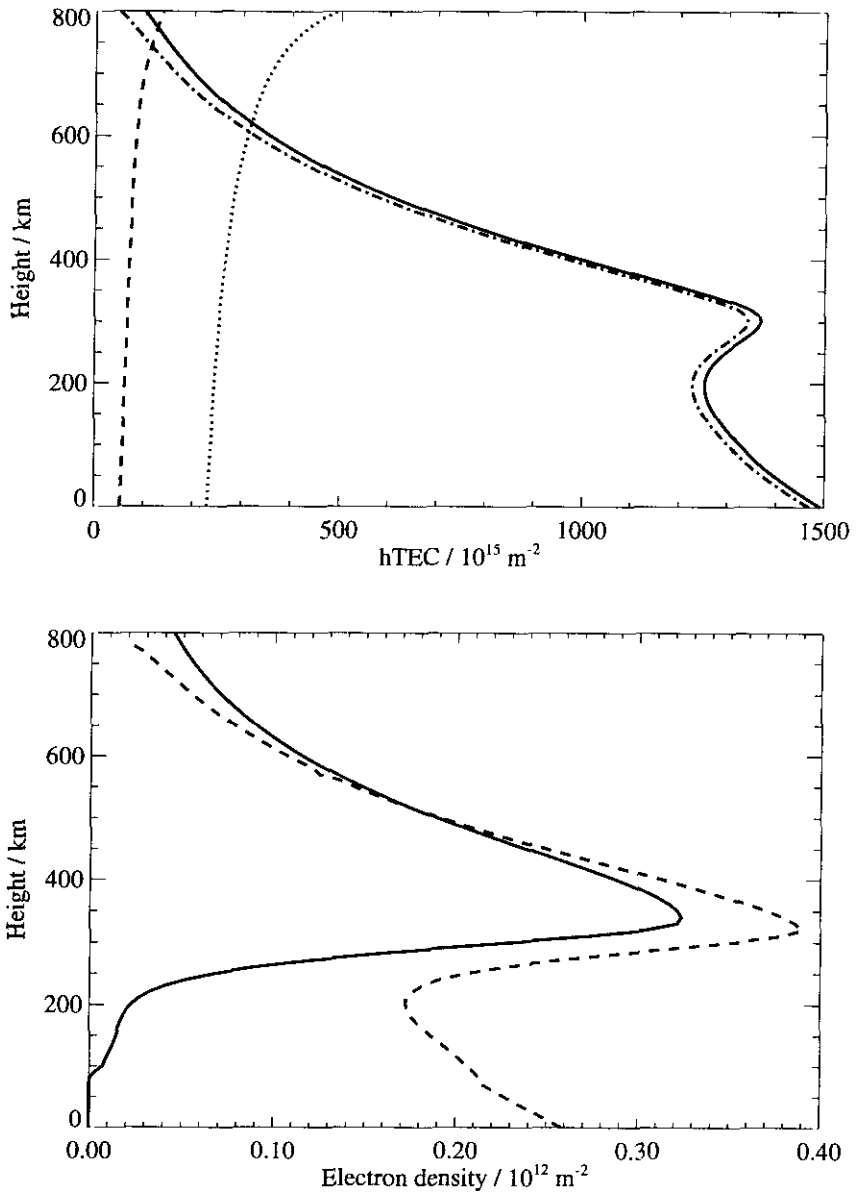


Figure 4. Upper panel: sTEC (multiplied by 100) of the plasmasphere from the GNS satellite to 2000 km (dashed line), sTEC (multiplied by 10) of the upper ionospheric part of the occultation between altitudes of 800 km and 2000 km (dotted line), sTEC of the ionosphere below 800 km (dashed-dotted line) and the total sTEC from GNS satellite to LEO satellite (solid line). Lower panel: height profile gained from inversion (dashed line) and directly from NeUoG-plas (solid line).

expect to gain meaningful results below about 200 km. For daytime conditions we have a good chance to gain results down to 100 km if electron densities in the E-F transition region are high enough and if the influence of horizontal gradients is weak enough (Leitinger et al., (1997b), Høeg et al., (1995)).

There are several possibilities for discretization of the inversion problem. To the knowledge of the authors two have been applied for GNSS - LEO occultations: (1) approximation of the height profile of electron density by a step curve (constant electron density in each pixel [shell]), (2) approximation of the height profile by a polygon (linear height dependence of electron density in each pixel).

If in the region of the occultation electron density depends on height only we can reconstruct the height profile to a high degree of accuracy and are limited only by discretization errors. «Weak» horizontal gradients of electron density can be tolerated.

Formally, the inversion results are «valid» even in the presence of «strong» horizontal gradients and we gain inversion profiles with a distinct maximum. However, the problem is the geophysical interpretation of the results.

For a systematic investigation let us assume a reconstruction plane perpendicular to the surface of the Earth on which the satellite to satellite rays are projected. We assume that this plane contains the ground occultation point. Furthermore we assume that the projections of the satellite to satellite rays are parallel to each other and that we can neglect the «smearing» in latitude and longitude of the ray perigees (assumption, that all ray perigee projections have the latitude and longitude of the ground occultation point). By interpolation we construct sTEC values for ray projections which are equidistant in height of the ray perigees. Then electron density along the rays can be considered to depend on height  $h$  and on a horizontal angular coordinate  $\psi$  ( $N_e = N_e(h, \psi)$ ). If  $\psi$  is counted from the ground occultation point all ray (projection) perigees have  $\psi = 0$ . The influence of the  $\psi$ -dependence of electron density on sTEC cancels out if  $N_e$  is an antimetric function of  $\psi$ , namely  $N_e(h, \psi) = N_e(h, -\psi)$ . Consequently, the  $\psi$  dependence of  $N_e$  has no influence on inversion results and inversion gives a good approximation to the height profile of electron density over the ground occultation point. (If measuring errors can be neglected the differences between inversion profile and true profile above the  $N_e$  maximum and especially just below the LEO orbit stem from data discretization and from inversion initialization only.) If, however, the condition  $N_e(h, \psi) = N_e(h, -\psi)$  is not fulfilled we might have the interpretation problems mentioned above and (geo)physically impossible negative values of electron density might appear in the lower part of the profile.

Because of colocation problems it is not possible to compare in detail occultation inversion results with height profiles from other experiments, e.g., from Incoherent Scatter. Therefore it is necessary to investigate the relation between a suitable height profile of electron density  $N_e(h)$  with the occultation inversion profile  $N_i(h)$  (index  $c$  for «comparison», index  $i$  for «inversion») by means of extensive model calculations (model based assessment studies) (Hochegger and Leitinger (1999), (2000)).

We have carried out such studies on the basis of the three dimensional ionosphere-plasmasphere model **NeUoG-plas** (for a description of the model see Leitinger and Kirchengast, (1997a), Leitinger et al., (1998a, b, 1999a)). For  $N_i(h)$  we took the «mid point profile» over the ground occultation point. Profile comparison needs strict guidelines and derivation of descriptive parameters from the profiles. Direct comparison of  $N_i$  against  $N_c$  makes no sense.

We have adopted the following four parameters.

1. The height of the absolute maximum of electron density  $h_{max}$ .
2. The value of the absolute maximum of electron density  $N_{max}$ .
3. A profile scale height around  $h = h_{max} + 250$  km and the slab thickness representative for the topside.
4. A weighted, averaged, relative deviation for the bottomside  $N_i(h)$  compared with  $N_c(h)$ .

We have calculated  $N_i(h)$  and  $N_c(h)$  from **NeUoG-plas** for every month of the year in two hours UT intervals and for two levels of solar activity (HSA:  $S_{10.7} = 200$  units, LSA:  $S_{10.7} = 80$  units) for about 250 occultation scenarios. The scenarios were distributed over four latitude zones, «high latitudes», «middle latitudes», «low latitudes» and «equatorial latitudes». The main purpose of the simulations carried out with **NeUoG-plas** was to investigate the dependence of the quality of the inversions on time (local time and season), on geographic location of the event and on environmental conditions (i.e., solar activity, geometry of the occultation scenario). Criteria were developed to assess the quality on a statistical basis. The comparison of inversion profiles and midpoint profiles gave the following results:

Dependence on local time and on season:

1. Inversion of occultation data is obviously a good tool to find the height of the F layer peak. Only less than 10% for each time interval missed the criterion of a height deviation of less than  $\pm 30$  km.
2. The shapes of the topside inversion profiles are very good during daytime but at nighttime they are more often «incorrect» for several time intervals.
3. The comparison of the bottom side profiles gives the largest differences with season and local time: In winter and during nighttime more than 60% of the cases failed the quality criterion but less than 5% in summer around noon.
4. For one of the most important properties of an electron density profile, namely the peak electron density (or the absolute values of the electron densities in general), problems occur. First the inversion results differ very often from the values of the midpoint profile. Secondly there are no clear «time structures», meaning that no simple time dependence of the quality of the results can be pointed out (see Fig. 5).

For the investigation of the influence of the geographic/geomagnetic location of an occultation the scenarios were split in two main groups: in middle

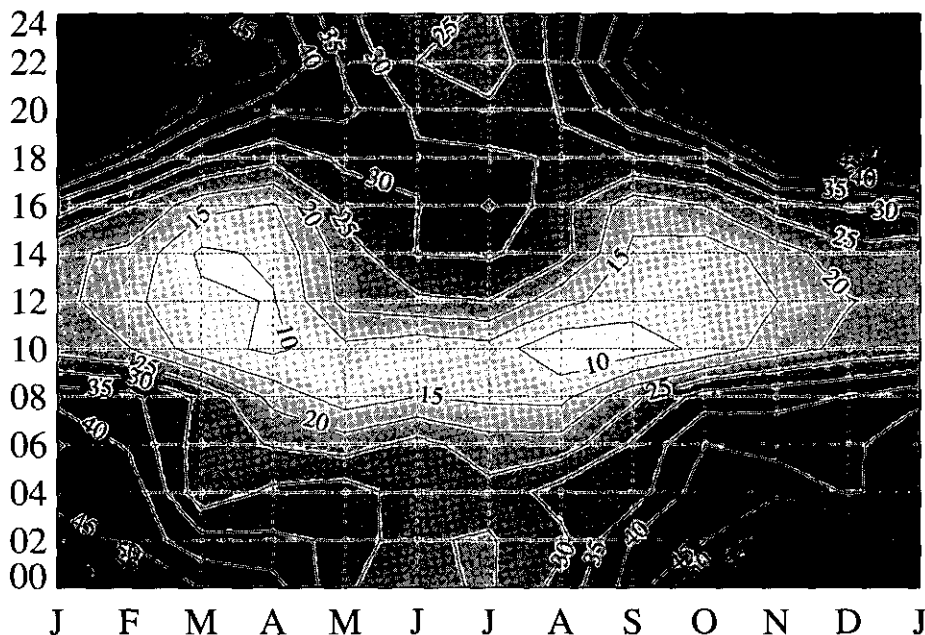


Figure 5. Profile comparison statistics. Comparison of peak electron density of the inversion profile,  $(N_m)_i$  with that of the profile above the ground occultation point,  $(N_m)_c$ . Data from all 248 occultation scenarios investigated under high solar activity conditions ( $S_{10.7} = 200$ ). Contour lines for the percentage of inversion profiles which failed the criterion  $|(N_m)_i - (N_m)_c| / (N_m)_c < 0.15$  in a LT vs. months of the year system. Dark shades: «bad» results, light shades: «good» results.

and high geographic (geomagnetic) latitudes and low and equatorial geomagnetic latitudes. This division led to the outcome, that for almost all comparison parameters middle and high latitude locations of the occultation events give better results than low latitude locations. Only the results in peak electron density are not of distinctly different quality for middle and low latitudes.

Comments on peak density results:

a) Even in the cases of «bad quality» (strong deviation of  $(N_m)_i$  from  $(N_m)_c$ ) we find NeUoG-plas peak density values identical to  $(N_m)_i$  in the geographic area of the occultation event (see below and compare Figures 6 to 8).

b) In view of the large spatial and temporal variability of  $N_m$  even «bad» inversion results can be extremely valuable in regions where we have no other data sources. Converting  $N_m$  into F2 layer critical frequency foF2 reduces the relative deviation between  $(foF2)_i$  and  $(foF2)_c$  to about half the relative deviation between the peak densities.

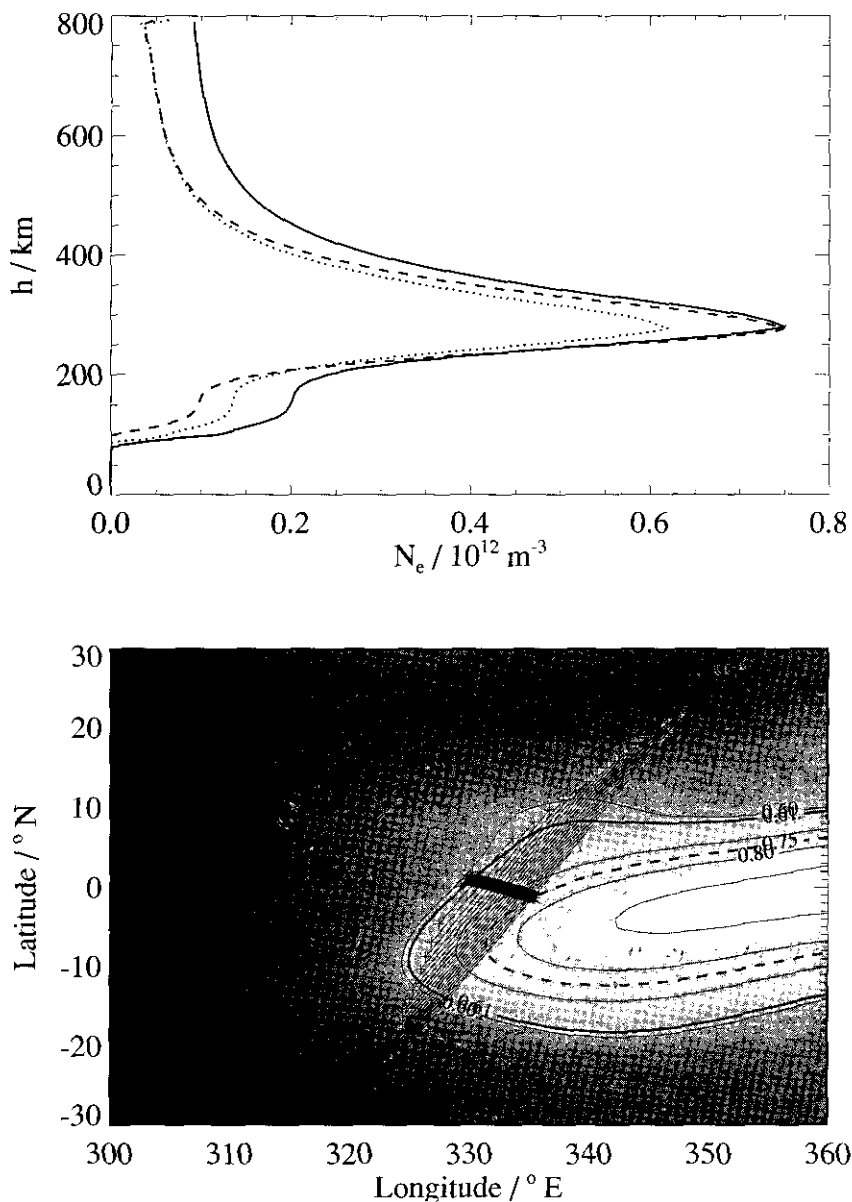


Figure 6. Comparison of height profiles of electron density and Scenario Map. Low solar activity conditions. Continuous line: profile above the ground occultation point; dotted line: profile from direct inversion; broken line: model assisted inversion ( $\alpha$  adjusted to match  $(N_m)_i$  to  $(N_m)_c$ ). Map: contour lines for  $N_m$  from NeUoG-plas in units of  $10^{12} \text{ m}^2$ . Trace of ray perigees (thick line) and selection of ray projections (lines between crosses). The ground occultation point is on the dashed contour line, the thick contour line marks  $(N_m)_r$ .

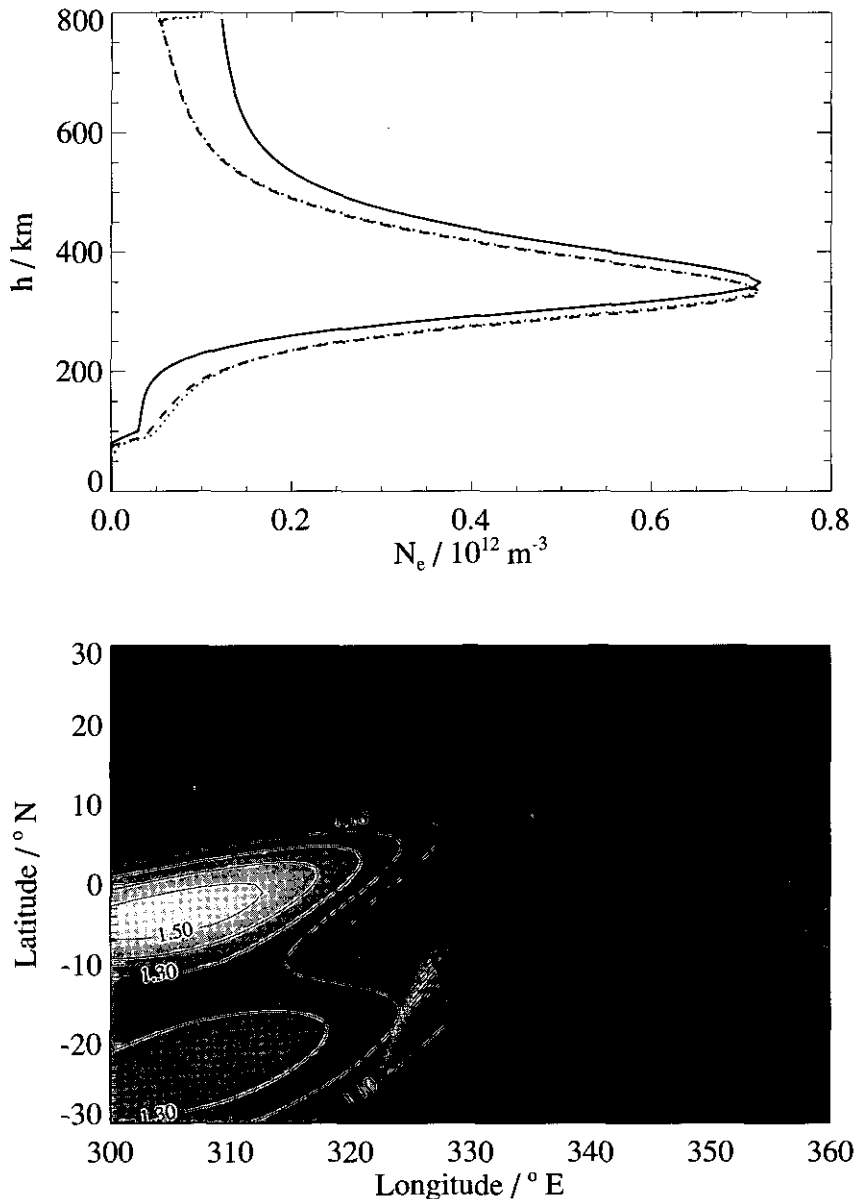


Figure 7. Comparison of height profiles of electron density and Scenario Map. Low solar activity conditions. Continuous line: profile above the ground occultation point; dotted line: profile from direct inversion; broken line: model assisted inversion ( $\alpha$  adjusted to match  $(N_m)_i$  to  $(N_m)_c$ ). Map: contour lines for  $N_m$  from **NeUoG-plas** in units of  $10^{12} \text{ m}^{-2}$ . Trace of ray perigees (thick line) and selection of ray projections (lines between crosses). The ground occultation point is on the dashed contour line, the thick contour line marks  $(N_m)_r$ .

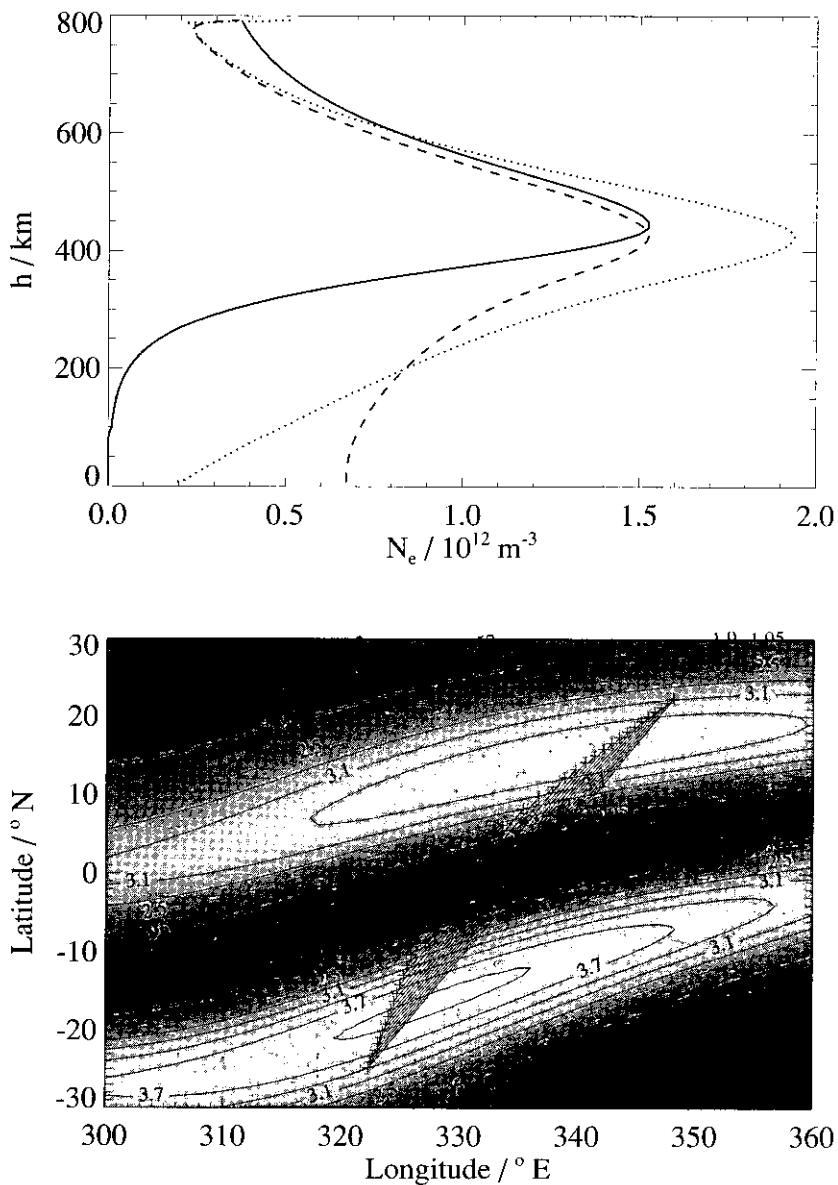


Figure 8. Comparison of height profiles of electron density and Scenario Map. High solar activity conditions. Continuous line: profile above the ground occultation point; dotted line: profile from direct inversion; broken line: model assisted inversion ( $\alpha$  adjusted to match  $(N_m)_i$  to  $(N_m)_e$ ). Map: contour lines for  $N_m$  from NeUoG(plus in units of  $10^{12} \text{ m}^{-2}$ ). Trace of ray perigees (thick line) and selection of ray projections (lines between crosses). The ground occultation point is on the dashed contour line, the thick contour line marks  $(N_m)_i$ .

## 2.2. Model assisted inversion

One type of use of satellite to satellite electron content is data assimilation into models. This involved process has not much in common with classical inversion.

There might be a simpler way to use some model information in inversion problems.

If we have enough additional information about the state of the ionosphere during an occultation event we can construct complicated models for the electron density distribution in the occultation region. Usually this is not the case and we have to be content with rather simple models for, e.g., relative maximal electron density as a (low resolution) function of  $\psi$ ,  $N_e / N_o = f(\psi)$ . (If we had a detailed 3D model of the actual electron density distribution we would not need to invert occultation data.)

We propose to input such model information by replacing the geometrical design matrix which consists of the lengths of the ray sections in each shell, by a matrix which consists of weighted lengths.

Original equation system (error vector omitted):

$$S \vec{N}_e = \vec{I}, \quad S = \begin{pmatrix} \dots\dots\dots \\ \dots S_{ij} \dots \\ \dots\dots\dots \end{pmatrix}, \quad S_{ij} = 2 \int_{s_{i-1}}^{s_i} ds, \quad S_{ij} = 0 \quad (i > j)$$

**S**: design matrix;  $\vec{N}_e$ : vector of electron densities (discretized height profile);  $\vec{I}$ : vector of sTEC values;  $i$  is the column index (indicating the «shells»),  $j$  the line index (indicating the «rays», the highest ray has  $j = 1$ , the ground occultation ray has  $j = n$ ). With the perigees of the rays,  $p_j$  and the height shell borders,

$$r_i = p_j + i (\Delta r) \text{ (for shells of equal thickness) we have } s_i = +\sqrt{r_i^2 - p_j^2}.$$

Introduction of the horizontal coordinate  $\psi$  and of a symmetric weight function  $g(\psi) = g(-\psi)$  leads us to the modified (weighted) design matrix  $S^*$  and we get

$$^* \vec{N}_e = \vec{I}, \quad S^* = \begin{pmatrix} \dots\dots\dots \\ \dots S_{ij}^* \dots \\ \dots\dots\dots \end{pmatrix}, \quad S_{ij}^* = 2 \int_{s_{i-1}}^{s_i} g(\psi) ds, \quad S_{ij}^* = 0 \quad (i > j)$$

$$(s_i = p_j \tan \psi_i \text{ and } ds = (p_j / \cos^2 \psi) d\psi).$$

Condition for the weights  $g(\psi)$  is that the total length between the LEO positions L and L\* (see Fig. 2) remains constant ( $S_{tot}^* = S_{tot}$ ):

$$\sum_{i=1}^j S_{ij}^* = \sum_{i=1}^j S_{ij} \quad \text{or} \quad \int_0^{S_{i=j}} g(\psi) ds = \int_0^{S_{i=j}} ds.$$

To demonstrate the method we use the simplest possible weight functions with an open parameter  $\alpha$

$$(a) \quad g(\psi) = \frac{1 + \alpha\psi^2}{g_o} \text{ [if } (N_m)_i \ll (N_m)_c \text{]},$$

$$(b) \quad g(\psi) = \frac{1}{1 + \alpha\psi^2} \frac{1}{g_o} \text{ [if } (N_m)_i \gg (N_m)_c \text{]}.$$

$g_o$  being the normalization factor which ensures that  $S_{tot}^* = S_{tot}$ . Furthermore, we have assumed the bare minimum of additional information to set a value for  $\alpha$ , namely knowledge of  $(N_m)_c$ .  $\alpha > 0$  is adapted in such a way that the model assisted inversion profile gets an  $(N_m)_i \doteq (N_m)_c$ . The most important application region for model assisted inversion is the vicinity of the dip equator or of a crest of the equatorial anomaly. If the ground occultation point is near the northern or southern crest we expect a direct inversion result with  $(N_m)_i \ll (N_m)_c$  and form (a) is needed for a compensating weight function (Fig. 6). On the other hand, if the ground occultation point is near the dip equator we expect a direct inversion result with  $(N_m)_i \gg (N_m)_c$  and form (b) is needed for the weight function. (Fig. 8).

For application of our model assisted inversion we propose to follow a strategy in steps:

1. Establish the approximate  $\psi$ -dependence of peak electron density below the ground occultation ray by means of nowcasting (instantaneous mapping) of ionosonde data or from a suitably adapted ionospheric model.
2. Apply direct inversion to the observed sTEC values.
3. Compare the resulting  $(N_m)_i$  with  $(N_m)_c$  from step (1) and make an «initial guess» for  $\alpha$ .
4. Apply model assisted inversion.
5. If necessary repeat steps (3) and (4) in an iterative algorithm.

Of course model assisted inversion is not restricted to additional information on  $N_m$  (or on foF2). It works equally well with any other type of single parameter description for the state of the F2 layer, e.g., with vertical electron content, with «equivalent slab thickness», with electron density in a fixed height near  $h_{max}$ .

### 3. PLASMASPHERIC ELECTRON CONTENT

The configuration C(3) provides rays from LEO locations to GNSS locations above the LEO orbit. These rays cross the uppermost ionosphere and most of the plasmasphere. If the LEO orbit is not too low one gains very valuable information on plasmaspheric electron contents and – by means of model assisted evaluation – on the electron density distribution in the plasmasphere. Under favorable conditions projections of the rays could even lead to tomographic reconstruction procedures.

Presently our knowledge on actual plasmaspheric electron density distributions is very scarce indeed and there is even a lack of data on plasmaspheric electron content for conditions of medium to high solar activity.

### 4. COMBINATION WITH DATA FROM OTHER SOURCES

#### 4.1. Data scenarios for tomography

Here we give only a brief description. More details with graphic displays are found in Leitinger, (1996), Høeg et al., (1995) and Leitinger et al., (1997a).

Four different scenarios for ionosphere tomography/imaging have been defined and investigated. The following order can be considered to be hierarchical.

**Scenario 1** is a combination of occultation with ground reception of dual-frequency beacon signals transmitted from the LEO satellite. A (truly) polar-orbiting satellite at a height around 1100 km would provide three to four useful passes per day (passes with a maximum ground elevation  $> 65^\circ$ ). More useful passes would exist at higher latitudes, but beyond a latitude of  $\pm 70^\circ$  the occultation properties are not suitable for tomographic reconstruction. (The inclination of the GPS satellites is  $55^\circ$ , and the inclination of the GLONASS satellites is  $65^\circ$ .) With both GPS and GLONASS reception on the LEO satellite, at least one «good» setting occultation can be found for each useful pass.

**Scenario 2** is a combination of occultation with ground based electron content data gained by means of propagation effects on the radio beacon signals transmitted from other LEOs. Presently the remaining active satellites of the former NNSS (U.S. Navy Navigation Satellite System) can be used but other beacons are planned for the future. With a slight degradation of requirements (colocation) one GNSS receiving satellite would provide two setting occultations per day useful for data combination with ground observations. Within a 30 minutes time interval the colocation of occultation rays (GNSS to LEO rays) and NNSS to ground rays is comparable to the situation found for ground to tomography: In the central part the occultation rays are in the space occupied by the NNSS to ground rays. NNSS signals now provide the main data source for «ionospheric tomography» [for an overview see Leitinger, (1996, 1999), and the original work referenced therein].

**Scenario 3** is a combination of occultation with GNSS reception by ground receivers. The GNSS satellites make a very slow «scan» only. If we do not allow time intervals longer than 30 minutes direct tomographic reconstruction of combined «space» and «ground» observations of GNSS signals would be feasible only with a very dense network of receiving stations. In 30 minutes a GNSS satellite moves about  $15^\circ$  in its orbit, which gives a ground ray bundle with a width of about  $20^\circ$ . Dense receiver spacing (about 50 km) would invert the geometry used from NNSS: a scarcity of transmitter positions but a sufficiently large number of receiver locations. Model-assisted imaging, however, needs receivers with a spacing of several hundred kilometers only. In some regions of the world (for example, in western Europe), such a network of receiving stations exists already now. The horizontal distribution of vertical electron content (from the ground to the height of the GNSS satellite) can be gained with sufficient accuracy and resolution by means of model-assisted nowcasting methods. Calibration is not necessary: Since electron content to the height of 20,000 km is contaminated by the contribution of the plasmasphere, an unknown additive constant has to be assumed. The (relative) vertical electron content is attributable to a 400-km trace corresponding roughly to the center ray of the GNSS-to-LEO occultation, the occultation providing vertical profile information. Both information sources can be merged for the reconstruction of a two—or three— dimensional electron density distributions (the «imaging» results).

**Scenario 4** is a combination of occultation with near-vertical TEC reconstructed from data gained from various other sources (navigation instruments like DORIS (Doppler orbitography and radiopositioning integrated by satellite), ionosonde profiles, and updated empirical models). This option has to be used in regions with insufficient density of ground receiver networks for scenarios 1 through 3 (over the oceans and presently, over wide areas in Africa and Asia, too). The (semi-) empirical vertical-TEC map is combined with the occultation information on the vertical profiles to yield «imaging» results. Typically, the horizontal resolution of this approach will not be better than the ionosphere occultation resolution (not below 500 km over the oceans).

## **4.2. Example for an occultation inversion**

We show one example for the inversion of «differential Doppler» data gained from the GPS signal reception by GPS/MET (see Ware et al., (1996)). The instrument was onboard MicroLab 1 (nearly circular orbit in a height around 750 km; inclination about  $70^\circ$ ). We have selected a «good» occultation in midlatitudes on October 22, 1995, 0735 UT (occultation 95/195/0063 in the list of the GPS/MET data center at UCAR, Boulder), which is illustrated in Fig. 9. The setting of the ray perigee through the ionosphere took about 6 minutes (from the height of MicroLab 1 to the ground).

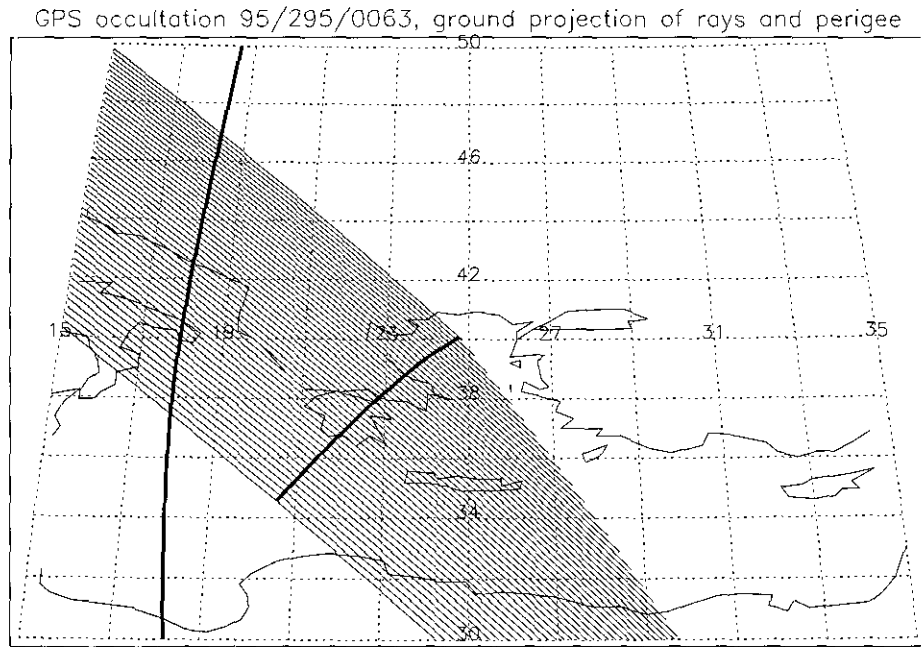


Figure 9. Map with ground projection of the ray perigee for the selected example of GPS to LEO occultation (heavy line) and of occultation rays (light lines, truncated at map borders) and of the ionospheric trace for an NNSS pass (heavy line). GPS BII-02 is in the northwest (subtrack position at end of occultation event:  $51.75^\circ$  N,  $266.96^\circ$  E), and MicroLab 1 is in the southwest (subtrack position at end of occultation event:  $12.05^\circ$  N,  $36.00^\circ$  E). The NNSS receiving stations are in the west of the map border (Gibilmanna:  $38.0^\circ$  N,  $13.4^\circ$  E).

The «ionospheric» GPS/MET data exist in intervals of 10 s. This resolution is marginally sufficient for inversion. Artificial resolution enhancement was gained by means of third-order interpolation. In this way the number of data were increased by a factor of 6. The data were extrapolated from the start height to the height of the MicroLab satellite. Then linear interpolation was used to gain phase data equidistant in height (100 intervals from the peak perigee height of 738.8 km to the ground). Fig. 10 (top) illustrates the P1-P2 phase difference data of the example case.

The «polygon» inversion technique described above was used to gain the horizontally averaged height profile of electron density. An initial oscillation of the solution damps out quickly (height range above 700 km in Fig. 10, bottom panel). The fluctuations in the height range 450-700 km reflect fluctuations in the P1-P2 phase data which are probably instrumental. In the example of Fig. 10 the results are useful down to a height of 80 km. It is interesting to note that an E layer appears despite the resolution limitation of the GPS/MET data.

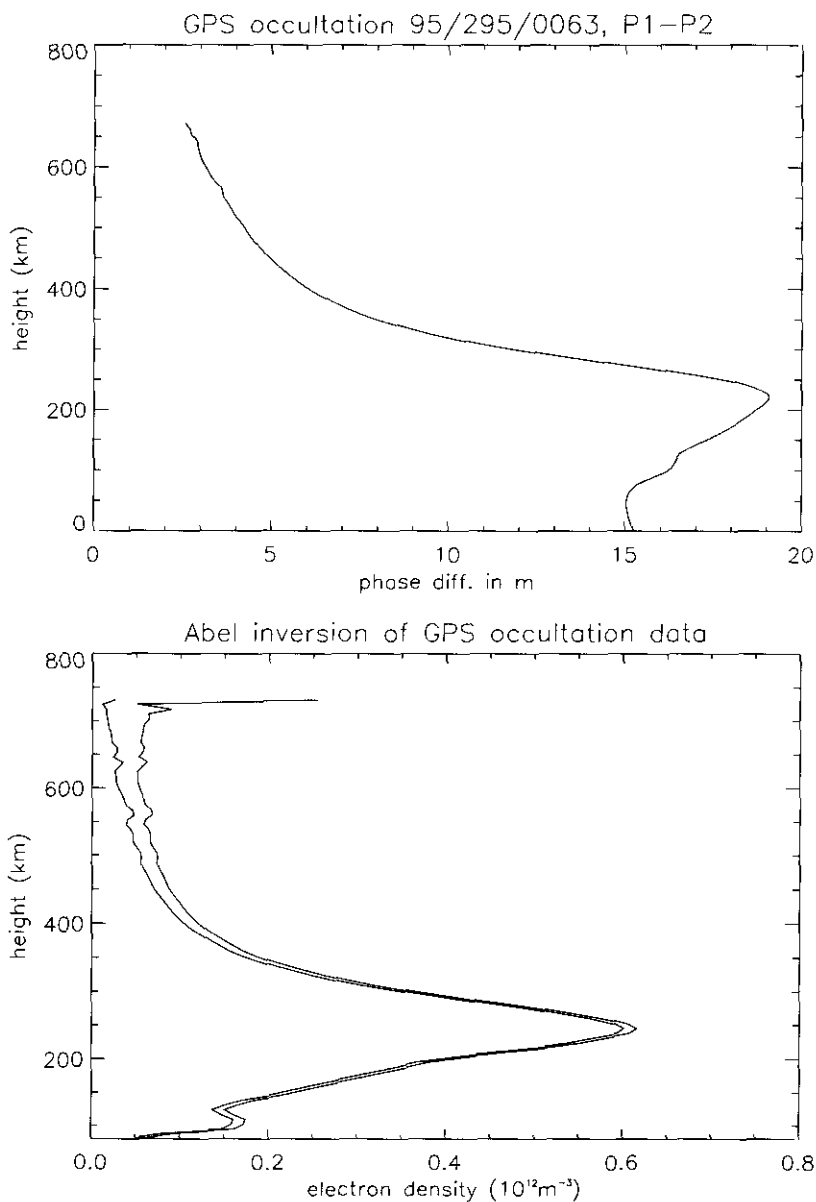


Figure 10. Height profiles of P1-P2 phase difference for the example GPS/MET occultation (top) and for the inversion results (bottom). The higher inversion values were gained without any correction for ionization above the LEO orbit. For the lower one, 90% of the electron content (P1-P2 difference value) for the top ray was subtracted before inversion. The resolution of the P1-P2 data was artificially enhanced by a factor of 6 using third-order interpolation.

Fig. 10 (bottom) shows two electron density profiles. The one with the higher values was gained directly from the P1-P2 phase difference as given in the relevant UCAR level 1 data. A correction for ionization above the MicroLab height was applied for the profile with the lower topside values: Before inversion a fixed value was subtracted from all data in this case. For this constant we chose 90% of the P1-P2 value at the MicroLab height. There is no doubt that the correction improves the profile at greater heights. The correction has nearly no effect on the profile below 350 km and does not influence the  $F_2$  and the  $E$  layer peaks in the result.

### 4.3. Example for a tomographic reconstruction

The following example (see 4.2) uses the combination of occultation data from GPS/Met (GPS occultation 95/295/0063) with electron content data from the ground reception of NNSS signals from three receiving stations (Gibilmanna/Sicily, Italy, L'Aquila, Italy and Graz, Austria). Since the NNSS receiving stations span a latitude of only 9 degrees model assisted construction of artificial slant TEC from observed vertical electron content was introduced for 6 additional ground locations.

The selected case is far from ideal. Colocation in space is not good (Fig. 9, the traces of the occultation rays intersect the trace of the «ionospheric points» on the rays from the ground stations to the NNSS satellite at angles around 45° (small angles would be best). The GPS BII-02 occultation was observed by GPS/Met at 07:35 UT, the NNSS pass was observed between 10:15 and 10:29 UT. The geographic/geometric situation was not good enough for a pure «Scenario 2» case (see above) therefore some model assistance was necessary. More for convenience than as a consequence of the geometric situation the 19°E meridian which is close to the subionospheric trace for the NNSS satellite was adopted as the reconstruction plane.

The procedure for tomographic reconstruction can be described as follows.

1. Horizontally averaged height profile. The inversion technique described in Leitinger et al., (1997a, b) was used to convert the carrier phase difference (P1-P2) data from the occultation observation into height profiles of electron density. The electron densities are «horizontal» averages from the orbit point of the LEO satellite to the point on the LEO to GNSS ray in the height of the LEO satellite. A modified electron density profile was prepared in the following way: removal of artifacts in the uppermost part and of the E layer trace by low pass filtering, cut off at 50 km, exponential continuation above 700 km.
2. Ground based data: Observed slant electron content. Slant electron content was used from 3 stations, namely Gibilmanna, Sicily (38.0°N, 14.0°E), L'Aquila, Italy (42.3°N, 13.4°E), and Graz, Austria (47.1°N, 15.5°E). The initial phase values (integration constants) were determined

by the «two stations method» (Leitinger et al., 1975) for Gibilmanna and L'Aquila. A least squares fit was used to attach the values for Graz to the combined Gibilmanna and L'Aquila values. Since the usual assumption of fixed mean ionospheric height  $h_i = 400$  km gave comparatively strong differences between the results in some latitude ranges, and since the occultation inversion gave a low F layer peak height of  $h_m = 230$  km, a latitude dependence was introduced for  $h_i = h_i(\phi)$ . The latitude dependence for  $h_m$  of the **NeUoG-plas** model ionosphere was approximated by  $h_m = 250 - (25/6)\delta + (5/60)\delta^2$ ,  $\delta$  being the latitude difference to the central latitude of  $48^\circ$  ( $h_m$  in km). ( $h_m$  of **NeUoG-plas** is identical to  $h_m$  of the CCIR maps (now sometimes called the ITU-R maps); model input parameters: month October, time 08 UT, longitude  $15^\circ$ E, solar activity R12 = 25). Finally,  $h_i(\phi) = h_m(\phi) + \Delta$  was adopted and a value of 50 km for  $\Delta$ . A latitude dependence of  $h_i$  needs an iterative evaluation process to gain vertical electron content from slant electron content.

3. Model assistance: Slant electron content for «artificial stations». Extensive model calculations have shown that tomographic reconstructions need rays to ground locations near the ends of the reconstruction space. Using the  $h_m = h_m(\phi)$  dependence described above and a linear extrapolation of vertical TEC for the region South of  $29^\circ$ N and North of  $54^\circ$ N, slant electron content was constructed for 6 artificial stations by projection in  $h_i$  (vert. TEC = (slant TEC)  $\cos \chi$ ,  $\chi$  being the zenith angle of the ray in  $h_i = h_m + \Delta$ ).

The tomography results were gained with the «parameter fitting method» (Leitinger et al., (1997a and b) which appears to be most suitable for marginal colocation and sparse data.

Truncated Singular Value Decomposition (SVD) was applied to find the coefficients of polynomials in the horizontal coordinate. The polynomials are multiplied with height profiles derived from the inversion results by inflation/deflation («scaling») and height shift as described in Leitinger et al., (1997b). For our example only 11 of 24 singular values were kept. Accordingly, the resulting two dimensional electron density distributions are realistic in the middle of the (very large) span of the horizontal coordinate only, namely for about  $\pm 12$  degrees from the center. Height profiles from the tomographic reconstruction are found in Fig. 11.

## 5. REMARKS ON OPERATIONAL ASPECTS

Since in the near future there will be GNSS receivers onboard many satellites we have to prepare for extensive use of the information. The ionospheric research community will need to carry out more assessment and comparison

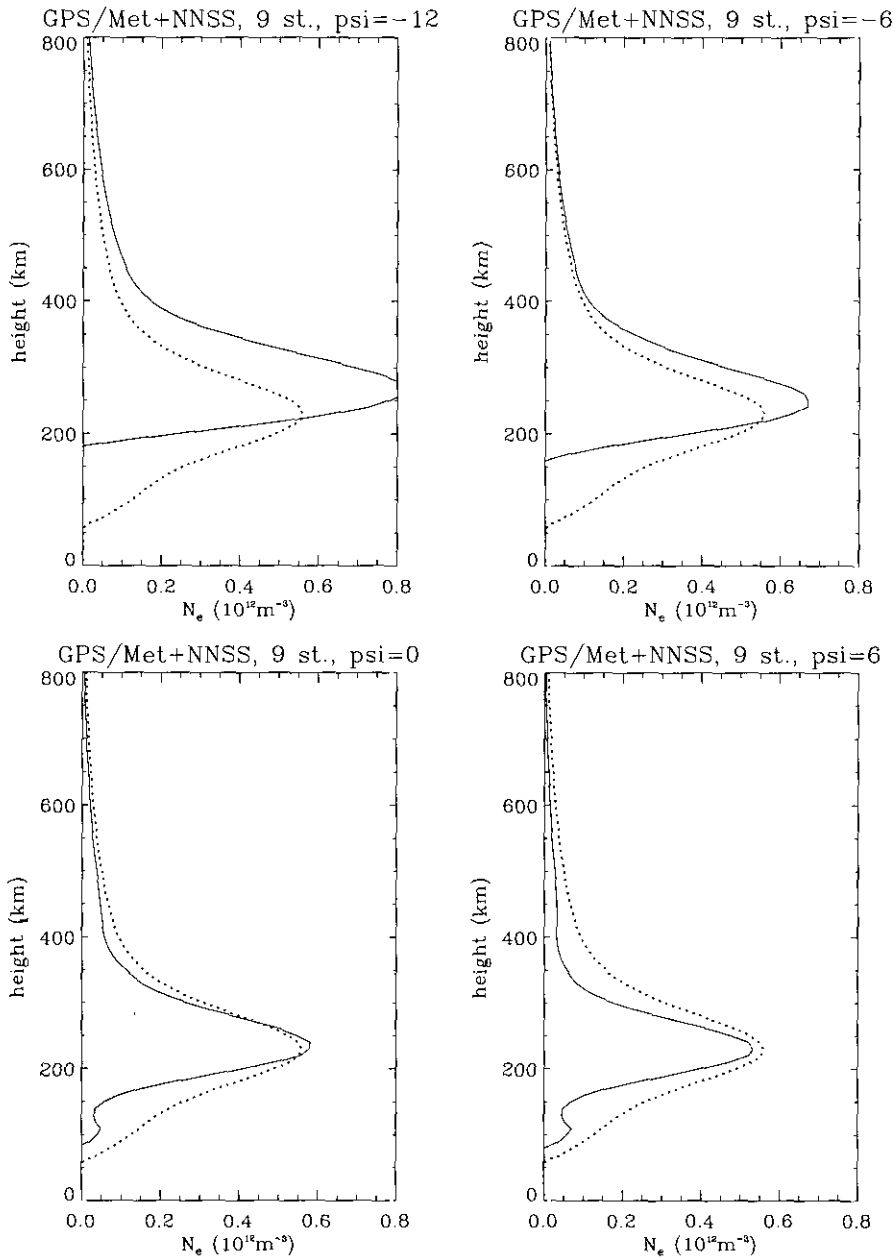


Figure 11. Tomographic reconstruction results. Height profiles of electron density compared with the GPS/Met inversion profile (dotted curves).  $\psi$  (psi) is the difference to the center latitude ( $48^\circ$  N). The results are considered representative for a longitude of  $19^\circ$  E (reconstruction plane =  $19^\circ$  E meridian).

studies to be able to incorporate the «novel» data into existing data bases. We have to prepare for «ionospheric» data retrieval, compression, storage and distribution systems. We have to preserve ionospheric physics and experience with ionospheric structures and phenomena otherwise there is an immediate danger that ionospheric «products» of doubtful quality will be fabricated by powerful industry related groups with the purpose to monopolize the «user market».

## REFERENCES

- HAIJ, G. A.; IBÁÑEZ-MEIER, R. KURSINSKI, E. R. and ROMANS, L. J. (1994): «Imaging the ionosphere with the Global Positioning System», *Int. J. Imaging Syst. Technol.*, **5**, 174-184.
- HAIJ, G. A., and ROMANS, L. J. (1998): «Ionospheric electron density profiles obtained with the Global Positioning System: Results from the GPS/MET experiment», *Radio Sci.*, **33**, 175-190.
- HOCHEGGER, G., and LEITINGER, R. (2000a): «Inversions of satellite to satellite electron content: Simulation studies with NeUoG-plas», *Phys. Chem. Earth (C)*, **25**, 353-357.
- HOCHEGGER, G., and LEITINGER, R. (2000b): «Simulation von GPS/GLONASS Okkultationen», *Kleinheubacher Ber.*, **43**, 256-262.
- HØEG, P., A.; HAUCHECORNE, G.; KIRCHENGAST, S.; SYNDERGAARD, B.; BELLOUL, R.; LEITINGER, and ROTHLEITNER, W. (1995): «Derivation of atmospheric properties using a radio occultation technique, ESA/ESTEC Contract Rep. 11024/94/NL/CN, DMI Sci. Rep. 95-4, ed. P. Høeg and S. Syndergaard, pp. 123-140, Danish Meteorol. Inst., Copenhagen.
- JAKOWSKI, N. (1999): «Capabilities of radio occultation measurements onboard LEO satellites for ionospheric monitoring and research, in: *Proc. 4th COST 251 Workshop*, ed.: A. Vernon, pp. 116-121, Funchal, Madeira, Portugal.
- KURSINSKI, E. R.; HAIJ, G. A.; BERTIGER, W. I.; LEROY, S. S.; MEEHAN, T. K.; ROMANS, L. J.; SCHOFIELD, J. T.; MCCLEAVE, D. J.; MELBOURNE, W. G.; THORNTON, C. L.; YOUNCK, T. P.; EYRE, J. T., and NAGATANI, R. N. (1996): «Initial results of radio occultation observations of Earth's atmosphere using the Global Positioning System», *Science*, **271**, 1107-1110.
- LEITINGER, R.; SCHMIDT, G., and TAURIAINEN, A. (1975): «An evaluation method combining the differential Doppler measurements from two stations that enables the calculation of the electron content of the ionosphere, *J. Geophysics (Zs. Geophysik)*, **41**, 201-213.
- LEITINGER, R. (1996): «Tomography», in *Modern Ionospheric Science*, ed. H. Kohl, R. Ruster and K. Schlegel), 346-370, Eur. Geophys. Soc., Katlenburg-Lindau, Germany.
- LEITINGER, R. (1996): «Transionospheric propagation studies: novel data sources», in: *Planetary Radio Emissions IV*, ed. H. O. Rucker, S. J. Bauer, A. Lecacheux, pp. 299-310 ÖAW Wien.
- LEITINGER, R., and KIRCHENGAST, G. (1997a): «Easy to use global and regional ionospheric models - a report on approaches used in Graz», *Acta Geodet. Geophys. Hung.*, **32**, 329-342.
- LEITINGER, R., and KIRCHENGAST, G. (1997b): «Inversion of the plasma signal in GNSS occultations - simulation studies and sample results», *Acta Geod. Geoph. Hung.*, **32**, 379-394.

- LEITINGER, R.; LADREITER, H.-P., and KIRCHENGAST, G. (1997a): «Ionosphere tomography combining data from spaceborne GNSS and ground-based NNSS reception», IMG/UoG Technical Report for ESA/ESTEC No. 1/1997, Graz.
- LEITINGER, R.; LADREITER, H.-P., and KIRCHENGAST, G. (1997b): «Ionosphere Tomography with data from Satellite Reception of Global Navigation Satellite System signals and ground reception of Navy Navigation Satellite System signals», *Radio Sci.*, **32**, 1657-1669.
- LEITINGER, R.; LADREITER, P., and KIRCHENGAST, G. (1997): «Ionosphärentomographie mit GNSS-Okkultationsdaten und ionosphärischen Elektroneninhalten», *Kleinheubacher Ber.*, **40**, 208-217.
- LEITINGER, R. (1998a): «A magnetic field aligned approach to model the topside F2 layer», *Adv. Space Res.*, **22**, 789-792.
- LEITINGER, R. (1998b): «NeUoG-plas - an easy to use global electron density model for the ionosphere and the plasmasphere», in: *Proc. 2nd COST 251 Workshop*, ed.: Y. Tulunay, pp. 140-150, Side, Turkey.
- LEITINGER, R. (1998c): «Ionospheric electron content, the European perspective», *Ann. di Geofisica*, **41**, 743-755.
- LEITINGER, R. (1999a): «Magnetic field aligned modeling for the upper F region and the magnetosphere», *Phys. Chem. Earth (C)*, **24**, 299-303.
- LEITINGER, R. (1999b): «Ionospheric Tomography». Ch. 24 of *Review of Radio Science 1996-1999*, ed. W. Ross Stone, pp. 581-623, International Union of Radio Science, Oxford University Press, ISBN 0 19 856571 2
- LEITINGER, R.; HOCHEGGER, G., and HAFNER, J. (1999): «NeUoG-plas ein flexibles Modell für transionosphärische Simulationsrechnungen», *Kleinheubacher Ber.*, **42**, 266-273.
- RIUS, A.; RUFFINI, G., and ROMEO, A. (1998): «Analysis of ionospheric electron density distribution from GPS/MET occultations», *IEEE Trans. Geosci. Remote Sensing*, **36**, 383-394.
- WARE, R.; EXNER, M.; FENG, D.; GORBUNOV, M.; HARDY, K.; HERMAN, B.; KUO, Y.; MEEHAN, T.; MELBOURNE, W.; ROCKEN, C.; SCHREINER, W.; SOKOLOVSKIY, S.; SOLHEIM, F.; ZOU, X.; ANTHES, V.; BUSINGER, S., and TRENBERTH, K. (1996): «GPS sounding of the atmosphere from low Earth orbit: Preliminary results», *Bull. Am. Meteorol. Soc.*, **77**, 19-40.